


Rapid RBE-Weighted Proton Radiation Dosimetry Risk Assessment

Technology in Cancer Research & Treatment
2016, Vol. 15(5) NPI-NP7
© The Author(s) 2015
Reprints and permission:
sagepub.com/journalsPermissions.nav
DOI: 10.1177/1533034615599313
tct.sagepub.com


Mohammad A. Z. Qutub, MS¹, Susan B. Klein, PhD¹,
and Jeffrey C. Buchsbaum, MD, PhD, AM^{1,2}

Abstract

Proton therapy dose is affected by relative biological effectiveness differently than X-ray therapies. The current clinically accepted weighting factor is 1.1 at all positions along the depth–dose profile. However, the relative biological effectiveness correlates with the linear energy transfer, cell or tissue type, and the dose per fraction causing variation of relative biological effectiveness along the depth–dose profile. In this article, we present a simple relative biological effectiveness-weighted treatment planning risk assessment algorithm in 2-dimensions and compare the results with those derived using the standard relative biological effectiveness of 1.1. The isodose distribution profiles for beams were accomplished using matrices that represent coplanar intersecting beams. These matrices were combined and contoured using MATLAB to achieve the distribution of dose. There are some important differences in dose distribution between the dose profiles resulting from the use of relative biological effectiveness = 1.1 and the empirically derived depth-dependent values of relative biological effectiveness. Significant hot spots of up to twice the intended dose are indicated in some beam configurations. This simple and rapid risk analysis could quickly evaluate the safety of various dose delivery schema.

Keywords

RBE, proton, dosimetry, safety, LET, linear energy transfer, relative biologic effect, radiation therapy, treatment planning

Abbreviations

RBE, relative biological effectiveness; SOBPs, spread out Bragg peak; DDF, distal dose falloff; IUHPTC, Indiana University Health Proton Therapy Center; PTV, planning target volume; LET, linear energy transfer; TPS, treatment planning systems

Received: December 22, 2014; Accepted: July 01, 2015.

Introduction

The advantage of proton beam therapy over conventional radiotherapy is an improvement in the conformality of the energy deposition inside the patient. This improvement arises from Bragg peak at the end of the proton range.^{1–3} High-density ionization events along with low energy proton tracks result in increased irreparable DNA damage that is the physical origin of an enhanced biological efficiency or relative biological effectiveness (RBE).⁴ The RBE can be measured by cell survival experiments or derived by biophysical models.⁵ Proton radiation has been shown to be more biologically effective for human cell killing compared with X-rays^{6,1} and so the standard of practice employs a dosimetric weighting factor between 1.1 and 1.2.^{7–9} However because RBE correlates with track structure, it increases near the end of range, at the Bragg peak. Relative biological effectiveness is derived from several Bragg peaks at several depths weighted to produce a flat physical dose with each peak contributing a pocket of densely ionizing track structures.

Several published studies support this intuition that from the midpoint to the distal side of spread out Bragg peak (SOBP), the RBE increases to a maximum of as much as 3 just^{10–15} beyond the distal dose falloff (DDF). The RBE value increases from 1.1 at the absorber entrance to as much as 1.6 at the midpoint of the SOBP¹¹ and to as much as 2.9 in the DDF.¹² Carabe *et al*¹⁶ suggested that when RBE weighing is used, the estimated range increases as much as 3 mm.

Variation in RBE over the SOBP could result in variations in biological dose that are not apparent when a uniform RBE of

¹ Department of Physics, Indiana University School of Arts and Sciences, Indianapolis, IN, USA

² Departments of Radiation Oncology, Pediatrics, and Neurological Surgery, Indiana University School of Medicine, Indianapolis, IN, USA

Corresponding Author:

Jeffery C. Buchsbaum, MD, PhD, AM, Department of Radiation Oncology, IU School of Medicine, 535 Barnhill Dr, RT041, Indianapolis, IN 46202, USA.
Email: jbuchsba@IUHealth.org

1.1 is used to calculate the treatment plan. This article presents a simple technique to enable visualization of proton biological dose in 2-dimensions and compares that with standard proton dose using a uniform RBE of 1.1. The isodose distribution profiles were accomplished using matrices that represent coplanar intersecting beams. These matrices were combined and contoured to represent the distribution of dose using standard RBE weighting values ($W_{\text{RBE}=1.1}$) or the depth-dependent weighting values of RBE ($W_{\text{RBE}=[\text{test}]}$).

Materials and Methods

Excel and MATLAB programs were used to construct biological isodose distributions of an artificial proton beam using either $W_{\text{RBE}=1.1}$ or the depth-dependent values $W_{\text{RBE}=[\text{test}]}$, and the results are compared herein. In this crude construct, the target is assumed to be a circular disk with a 30 mm diameter with a matching SOBP. Measurements of depth-dose profiles taken at Indiana University Health Proton Therapy Center (IUHPTC) by Britten *et al*¹⁷ were modified for this performance test of the method for determining boundary parameters for safe dose delivery. This data set was selected not because it was representative of published works reporting proton RBE, but because the data were collected in-house under standard beam conditions used for dosimetry at IUHPTC. The Britten tumor cell clonogenic assays were performed at 33.9, 53.9, 58.6, and 60.9 mm depths along a beam with incident energy of 87 MeV with an SOBP of 46 mm.

The data for this test of the methodology were mathematically derived. The RBE values were scaled using a relative depth within the 30 mm SOBP. The published data were used to establish percentage depth positions of RBE data.

The scaled position of each point of interest within the SOBP ($X(n)$) is calculated:

$$X(n) \text{ cm} = \frac{X_{\text{cm}} \times (\text{the depth within the original SOBP} - 1.4\text{cm})}{4.5\text{cm}} + X(n - 1) \quad (1)$$

where $X(n - 1)$ is the depth in cm of 90% maximum dose, proximal end of the SOBP of interest and X is the length in cm of the SOBP of interest. The scaling factors 1.4 and 4.5 cm isolate the modification to within the SOBP.

Two dosimetry profiles were constructed for comparison. In addition to the isodose profile generated using the standard weighting factor $W_{\text{RBE}=1.1}$, a position sensitive biological isodose profile was calculated using the following relationship:

$$D_{\text{RBE}}(\text{RBE} = \text{ref}[16]) = \frac{D_{\text{RBE}}(\text{RBE} = 1.1)}{1.1} \times W_{\text{RBE}=[\text{test}]} \quad (2)$$

where $D_{\text{RBE}}(\text{RBE} = \text{ref}[16])$ is the dose at a given point calculated by weighting the physical dose (the standard biological dose divided by 1.1) at that point by the appropriate weighting factor derived from Britten *et al* $W_{\text{RBE}=[\text{test}]}$. The standard biological dose is represented as $D_{\text{RBE}}(\text{RBE} = 1.1)$

Microsoft Excel 2013 was used to develop a matrix. Each column of the matrix contains the values of the X-ray dose present in y for the transverse section of the treatment object and each row contains the values of the X-ray dose present in x for the transverse section. Each element in the matrix represents the value of the fractional dose taken from the digital data of the dose-depth profile.

The transverse section of the treatment object is assumed to be a 9 cm diameter circle, and the planning target volume (PTV) is a concentric circle with a 30 mm diameter. Thus, the matrix transverse section is $89 \times 89 \text{ mm}^2$. The width of the modeled proton beam is 30 mm and it is constructed within the matrix with the planned orientation. The matrix is filled manually for beam angles of 0° , 90° , 180° , 225° , 270° , and 315° , for $W_{\text{RBE}=1.1}$ and $W_{\text{RBE}=[\text{test}]}$. There are 12 matrices total. The matrices prepared in Excel are uploaded to MATLAB R2013a manually.¹⁸ The total to each cell of the matrix is achieved by summing the contribution from each intersecting beam. The data are then normalized to 100% at maximum dose. After the image of the isodose distribution is captured, the “colorbar” is used to adjust the isodose distribution weight. “Custom” was selected within the color map menu to set the maximum color indicator at the maximum dose.

Results

A simple visualization of biological dose was created using MatLab to construct a circular PTV within a homogeneous circular treatment target volume (TTV) in 2-dimensional space. The standard RBE of 1.1 was assumed throughout an SOBP that was adjusted to cover the 3.0 cm diameter PTV. This model was used to compare a variety of beam configurations designed to provide an even dose distribution at $\text{RBE} = 1.1$, planned to the 90% isodose over the PTV. These plans were then compared with isodose profiles that would result from applying the depth dependent, 10% survival RBE values reported by Britten *et al*¹⁷ under the same conditions. Because the SOBP extent depends on the PTV, as the SOBP extent varies the entrance percentage dose will change and the midpoint depth will vary. The data used to test the model were rescaled at the entrance dose and the positions of the $W_{\text{RBE}=[\text{test}]}$ according to the methods given. It therefore does not represent empirical data but rather an approximation used to test the method described herein. Adjusting the values provided by Britten, the relative dose at the entrance of a 30 mm SOBP will be 0.61 and the new positions of $W_{\text{RBE}=[\text{test}]}$ as shown in Figure 1. The biologically weighted relative dose using the rescaled values for a 30 mm SOBP with an incident energy of 87 MeV is compared with the standard relative dose ($W_{\text{RBE}=1.1}$). For all plan comparisons, the dose at the proximal edge of a PTV was normalized for each beam as shown in Figure 1 demonstrated by the red and blue lines overlapping.

The modeled plan represents a transverse section of a 9 cm diameter circular TTV with a concentric PTV of 3 cm diameter, intersected by proton beams (30 mm width, 80% to 80%). Two, 3, 4, 5, and 6 beams, with 45° , 90° , 135° , and 180° separation,

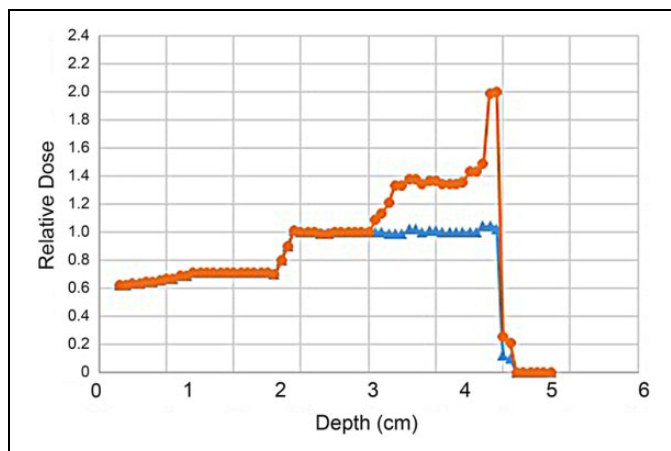


Figure 1. The 30 mm spread out Bragg peak (SOBP) depth–dose profiles with $W_{RBE=1.1}$ (Δ) and $W_{RBE=[test]}$ (\circ). Incident proton energy 87 MeV. Points are connected by linear extrapolation.

intersect the PTV such that their DDF is at the distal side of the PTV with an SOBP of 30 mm (90% to 90%). The dose distributions for these beams were first calculated using the standard uniform $W_{RBE=1.1}$. The dose distributions were then recalculated using the Britten *et al*'s $W_{RBE=[test]}$ values for Hep2 cells, scaled to 30 mm. These $W_{RBE=[test]}$ values are depth and energy dependent and vary along the SOBP.

When the $W_{RBE=[test]}$ values are applied to the dose calculation using a 45° angle between the 2 beams, a hot spot appears at the distal edges of both beams (Figure 2). The biological dose at the hot spot is 100% greater than the intended dose calculated using uniform $W_{RBE=1.1}$. About 30% excess dose is delivered to nearly half of the treatment volume due to the increased RBE in the second half of the SOBP. When parallel opposed beams are used (Figure 3), this increase in RBE mid-SOBP results in a linear band of increased dose of about 35% mid-PTV. In this case, the distal hot spots on either side of the PTV “box” are 45% greater than the planned dose based on $RBE = 1.1$. In general, the corrected $W_{RBE=[test]}$ relative dose in the mid-distal SOBP beam edges is between 20% and 80% greater than the uniform $W_{RBE=1.1}$ calculated doses.

If a third field is added to the parallel opposed plan such that the separation is 90° between the beams, the influence of the increased RBE over the second half of the SOBP of the third beam can be visualized readily in the increased dose throughout the upper half of the box. The difference between the calculated dose distributions indicates both an increase in the excess dose over that produced by 2 opposing beams at the distal periphery of the 3 beams and increased dose to more than half of the treatment volume. For 3 beams with a 45° angle between them, the hot spot of the corrected $W_{RBE=[test]}$ relative dose is concentrated at the distal corners. Nonetheless, the dose to the central tissue within the PTV may be approximately 30% greater than planned. At the hot spots, the biological dose is 70% greater than that calculated using the uniform $W_{RBE=1.1}$. The dose distributions using a uniform $W_{RBE=1.1}$ or corrected $W_{RBE=[test]}$ have no considerable differences at the PTV

entrance. Lesser increases in dose ranging between 20% and 60% can be seen at the proximal corners.

When the angle between 3 modeled beams is 90°, the hot spot visualized when using the corrected $W_{RBE=[test]}$ dose is greater by 55% than the uniform $W_{RBE=1.1}$ dose. In general, the dose distribution using $W_{RBE=[test]}$ values is 15% to 45% higher than the standard $W_{RBE=1.1}$ dose.

Adding a fourth field to the 45° offsets reduces the area encompassed by the 30% dose excess, but the hot spots created by incorporating the corrected $W_{RBE=[test]}$ are 60% greater than the dose predicted by the uniform $W_{RBE=1.1}$. In general, the $W_{RBE=[test]}$ -weighted relative dose for intersection corners are between 15% and 55% greater than the $W_{RBE=1.1}$ dose. When the angle between each of 4 beams is increased to 90°, the $W_{RBE=[test]}$ corrected dose at the hot spots is 45% greater than the uniform $W_{RBE=1.1}$ dose (Figure 4). A hot spot is now apparent in the center of the PTV. In general, the dose distribution using corrected $W_{RBE=[test]}$ is between 10% and 40% greater than the uniform $W_{RBE=1.1}$.

Additional fields are not effective at reducing either the distal or central hot spots. The configurations for 5 and 6 beam distributions (Figure 5) display corrected $W_{RBE=[test]}$ hot spots, 40% to 45% greater than the uniform $W_{RBE=1.1}$ dose. In general, the corrected $W_{RBE=[test]}$ relative doses are 15% to 40% higher than the uniform $W_{RBE=1.1}$.

Discussion and Conclusion

The current standard of practice in proton therapy clinics is to use a biological effectiveness correction factor based on empirical evidence⁸ to account for the increased RBE of proton radiation over X-ray radiation. This weighting factor, $W_{RBE=1.1}$, is likely not accurate for all cases where the incident beam energy and SOBP extent may vary. Empirical evidence would indicate a dependence of RBE on linear energy transfer (LET) that is known to vary with depth along the proton track. Several investigations have measured variation in RBE with depth in a biological absorber for both *in vitro*^{10,18-26} and *in vivo*,²⁷⁻³¹ systems. Experimental conditions have used various cell lines with differences in sampling along the SOBP, initial beam energy, RBE calculation method, tissue type, and LET estimation. *In vitro* RBE values also depend upon the survival level at which they are measured. Variations in the values of RBE applied to planning algorithms will influence the effective dose distributions. The application of various published RBE values will result in different biological dose outcomes. Clinicians should be judicious regarding the selection of empirical data used to model the clinical situation when applying this method for risk assessment. We have elected to modify the values published by Britten *et al*¹⁷ for illustrative purposes in this article, though this simple technique can be used to evaluate potential isodose difference plots for any appropriate weighting factors of interest. The Britten data were selected not because it was representative of published works reporting proton RBE, but because the data were collected in-house under standard beam conditions used for dosimetry at

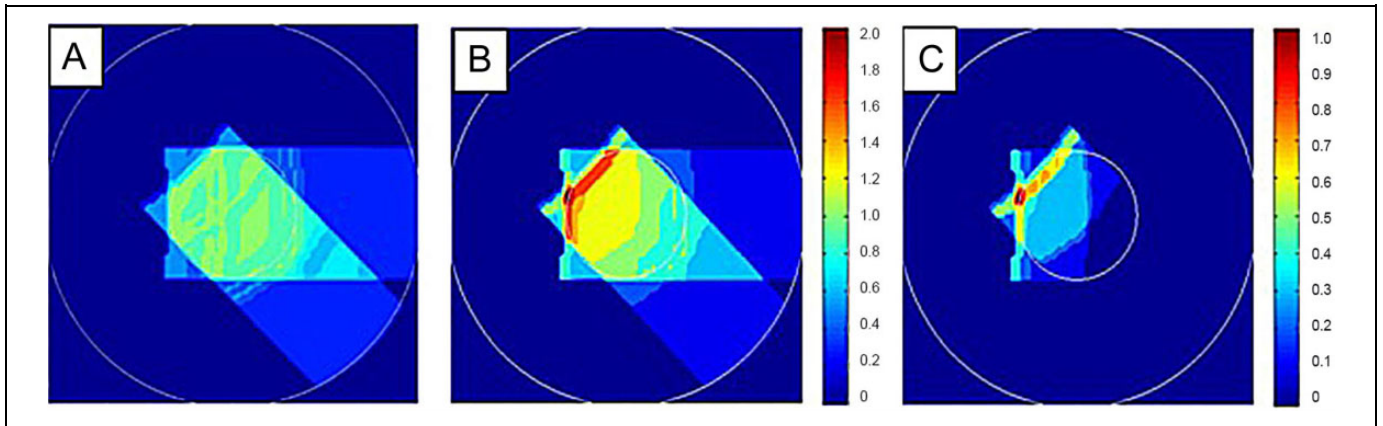


Figure 2. Isodose distribution profiles of 2 proton beams with 45° of separation (0° and 315°) range = 60 mm, spread out Bragg peak (SOBP) = 30 mm. A, $W_{RBE=1.1}$, B, $W_{RBE=[test]}$, and C, the difference in isodose distribution. The planning target volume (PTV) is 30 mm in diameter and the transverse section is 90 mm in diameter.

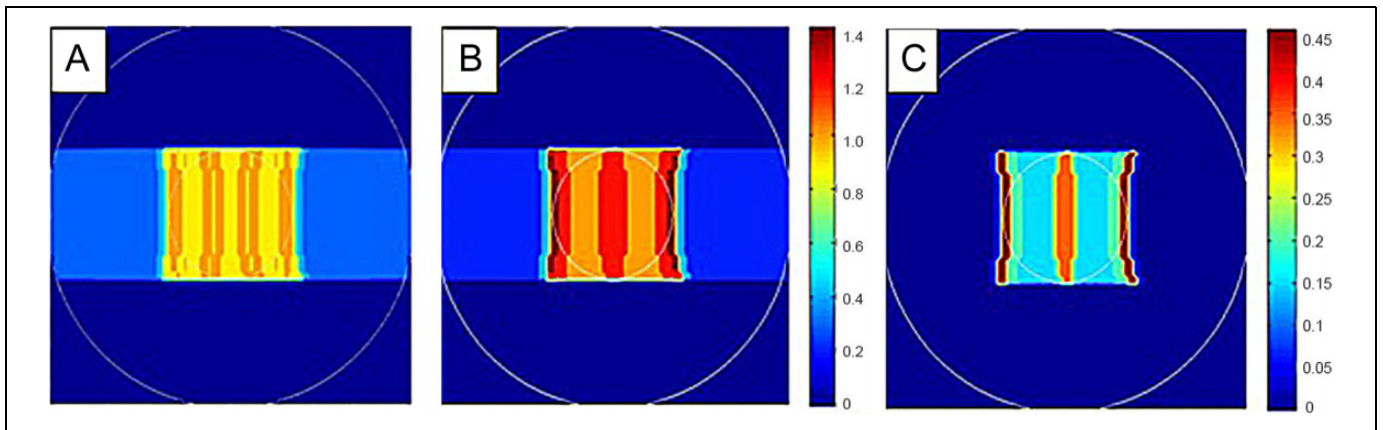


Figure 3. Isodose distribution profile of parallel opposed proton beams at 0° and 180°. A, $W_{RBE=1.1}$, B, $W_{RBE=[ref[16]]}$, and C, the difference in isodose distribution.

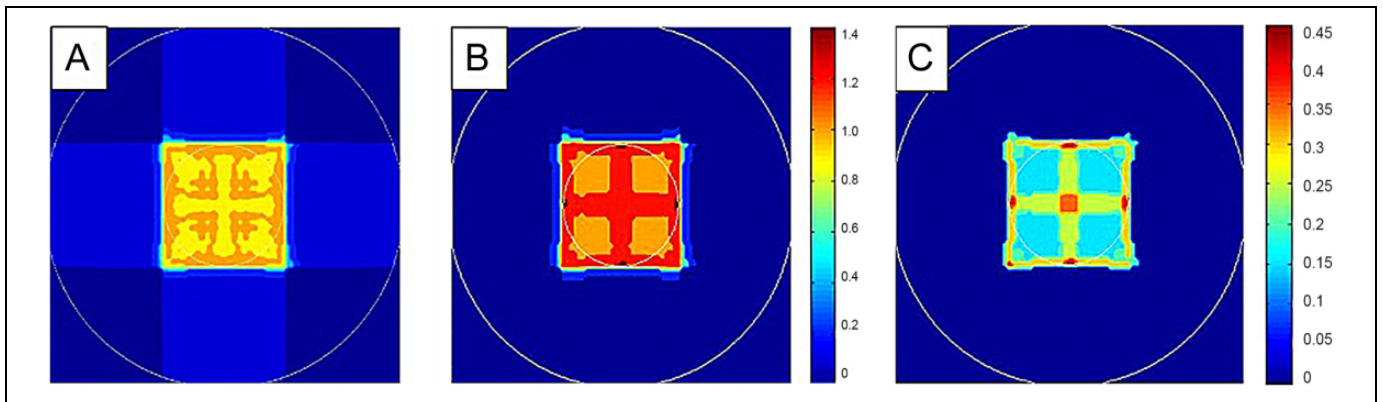


Figure 4. Isodose distribution profile of 4 proton beams at 0°, 90°, 180°, and 270°. A, $W_{RBE=1.1}$, B, $W_{RBE=[test]}$, and C, the difference in isodose distribution.

IUHPTC. The application of this method in a clinical setting would require, using plan specific initial beam energies, SOBP parameters and appropriate compensated ranges as well as

appropriate empirically derived RBE values. The calculated parameters used herein were generated specifically for the purpose of illustrating the risk assessment algorithm.

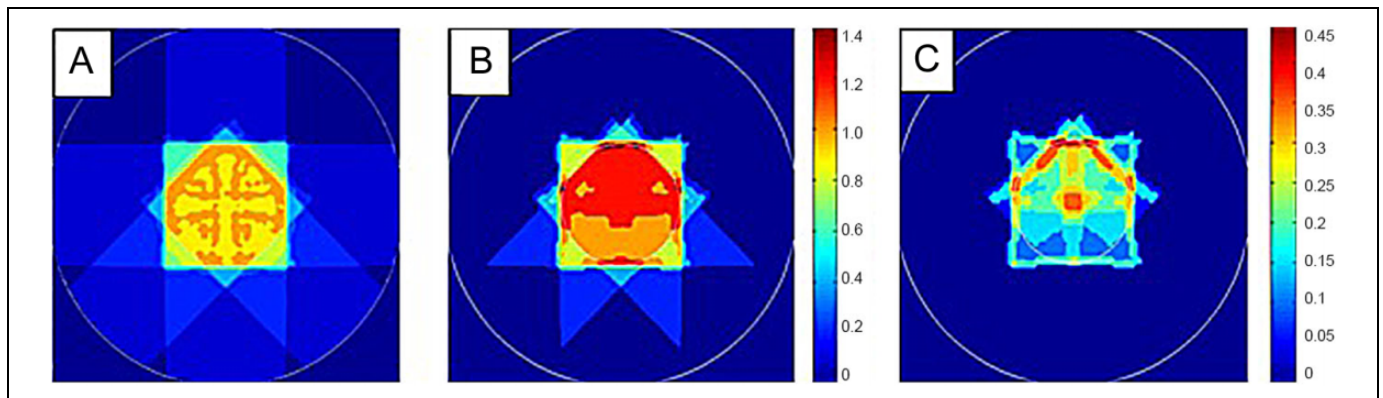


Figure 5. Isodose distribution profile of 6 proton beams with 0° , 90° , 180° , 225° , 270° , and 315° . A, $W_{\text{RBE}}=1.1$, B, $W_{\text{RBE}}=[\text{test}]$, and C, the difference in isodose distribution.

The application of weighting factors not equal to 1.1 indicates hot or cold spots in the dose distribution within the target or excessive dose to healthy tissue. The techniques developed herein disclose some significant differences between the clinically applied $W_{\text{RBE}}=1.1$ dose distributions and the dose distributions that would be derived from the empirically determined W_{RBE} values. Variations among reported RBE values^{31–33} and between values derived from *in vitro* and *in vivo* studies represent an uncertainty in the biological dose that is being delivered clinically.

The variation in biological dose depends on the number of proton fields and the angles between them because the increased W_{RBE} occurs not only at the distal falloff but also along the SOBP. Our isodose profile figures suggest that the increase in W_{RBE} can result in hot spots of up to 100% of the prescribed dose for 2 beams with 45° between them (Figure 2), about 80% for 3 beams with 45° between them, and about 60% for 4 beam boxes (Figure 4). In general, the least worrisome distributions used 5 or 6 beams where the increased dose spread out relatively evenly inside the PTV, and the increase in dose was less than 40%. The more dangerous distributions appeared when 2 and 3 beams were created with 45° between beams since the hot spots concentrated in relatively small areas inside the PTV with a dose increase of up to 80% to 100%.

What is presented is a simple method for evaluating potential risk. This method can be used to rapidly assess the risk of any clinically planned treatment. For argument's sake, suppose that a maximum increase in biological dose of 25% greater than the dose determined using the standard software $W_{\text{RBE}}=1.1$ is clinically acceptable. Then any MATLAB-derived distribution profiles incorporating the planned parameters resulting in biological doses greater than planned +25% should be disallowed and the plan should be adjusted to reduce all uncertainties in biological dose to less than $\pm 25\%$ of $W_{\text{RBE}}=1.1$ dose.

Important factors that cannot be considered in this work because of their complexity include the anatomical placement and extent of the hot spot. For example, a hot spot aligned with a particularly susceptible tissue mass may result in higher risk. Several factors are patient and organ specific and lie outside the

scope of this work. Mitigation could be accomplished by slightly reducing the incident beam energy for some number of fractions as suggested by Buchsbaum *et al.*,³⁴ which pulls the end-of-range back from the edge of the PTV. Fortunately, uncertainties in patient setup and organ motion during treatment also contribute to a smearing effect and probably are responsible for preventing the potential untoward patient outcomes that might be predicted by the results presented herein. Although there are occasional anecdotal reports of unanticipated treatment-related injury to patients that implicate a possible delivery of acute punctate excess dose, no evidence exists for systematic damage associated with current proton therapy clinical protocols using the standard $W_{\text{RBE}}=1.1$ weighting factor.

Nonetheless, this work and the work of others^{8,14,17,30,35} make it clear that although we have an excellent understanding of the dose deposition physics of charged particle irradiation, we do not have sufficient understanding of the biological responses to that energy absorption. Because it is the biological response that is driving the clinical prognosis, this uncertainty is quite compelling.

In time, this methodology could be optimized and placed into treatment planning scenarios much like we use raw dose in the current process. Treatment planning systems (TPSs) currently are beginning to look at biologic optimization. What we envision as this project's ultimate use is the real-time generation of biologic dose in a TPS that can then be modulated via the allowance of nonlinear SOBP shape so as to make biologic dose more homogeneous. This, in essence, means inverting the current process of optimizing physical dose and accepting biologic dose to optimize biological dose and accepting physical dose. This would have to be done over time as the work to date in clinical radiation oncology is completely based on physical dose. It would also require a major change in how we define beams as we would be very unlikely to use SOBPs designed to have a flat physical dose as we currently do. Ultimately, the delivery of proton treatment plans would be made up of series of unique mixtures of pristine Bragg peaks rather than SOBPs. In the end, the visualization of biologic dose is crucial in providing the safest possible treatment plans to patients.

Declaration of Conflicting Interests

The author(s) declared no potential conflicts of interest with respect to the research, authorship, and/or publication of this article.

Funding

The author(s) received no financial support for the research, authorship, and/or publication of this article.

References

1. Miller DW. A review of proton beam radiation therapy. *Med Phys*. 1995;22(11 pt 2):1943-1954.
2. Bethe HA. Molier's theory of small-angle multiple scattering of fast charged particles. *Rev Mod Phys*. 1963;35(2):231-313.
3. Yock T, Esty B, DeLaney TF, Tarbell NJ. Pediatric tumours. In: Delaney TF, Kooy HM, eds. *Proton and Charged Particle Radiotherapy*. Philadelphia, PA: Lippincott Williams & Wilkins; 2008; 125-130.
4. Wambersie A. RBE, reference RBE and clinical RBE: applications of these concepts in hadron therapy. *Strahlenther Onkol*. 1999;175(2):39-43.
5. Hall EJ, Giaccia AJ. *Radiobiology for the Radiologist*, 7th ed. Philadelphia, PA: Lippincott Williams & Wilkins; 2006:35-53.
6. Raju MR, Amols HI, Bain E, et al. A heavy charged particle comparative study III: OER and RBE. *Br J Radiol*. 1978; 51(609):712-719.
7. Skarsgard L. Radiobiology with heavy charged particles: a historical review. *Phys Med*. 1998;14(suppl 1):1-19.
8. Paganetti H, Niemierko A, Ancukiewicz M, et al. Relative biological effectiveness (RBE) values for proton beam therapy. *Int J Radiat Oncol*. 2002;53(2):407-421.
9. International Commission on Radiation Units and Measurements. *Prescribing, Recording and Reporting Proton-Beam Therapy (ICRU report 78)*. Bethesda, MD: ICRU; 2007.
10. Courdi A, Brassart N, Hérault J, Chauvel P. The depth-dependent radiation response of human melanoma cells exposed to 65 MeV protons. *Br J Radiol*. 1994;67(800):800-804.
11. Belli M, Cera F, Cherubini R, et al. RBE-LET relationships for cell inactivation and mutation induced by low energy protons in V79 cells: further results at the LNL facility. *Int J Radiat Biol*. 1998;74(4):501-509.
12. Bettega D, Calzolari P, Marchesini R. Inactivation of C3H10T1/2 cells by low energy protons and deuterons. *Int J Radiat Biol*. 1998;73(3):303-309.
13. Frese MC, Wilkens JJ, Huber PE, Jensen AD, Oelfke U, Taheri-Kadkhoda Z. Application of constant vs. variable relative biological effectiveness in treatment planning of intensity-modulated proton therapy. *Int J Radiat Oncol*. 2011;79(1):80-88.
14. Frese MC, Yu VK, Stewart RD, Carlson DJ. A Mechanism-based approach to predict the relative biological effectiveness of protons and carbon ions in radiation therapy. *Int J Radiat Oncol*. 2012; 83(1):442-450.
15. Wroe A, Schulte R, Fazzi A, Pola A, Agosteo S, Rosenfeld A. RBE estimation of proton radiation fields using a ΔE -E telescope. *Med Phys*. 2009;36(10):4486-4494.
16. Carabe A, Moteabbed M, Depauw N, Schuemann J, Paganetti H. Range uncertainty in proton therapy due to variable biological effectiveness. *Phys Med Biol*. 2012;57(5):1159.
17. Britten RA, Nazaryan V, Davis LK, et al. Variations in the RBE for cell killing along the depth-dose profile of a modulated proton therapy beam. *Radiat Res*. 2013;179(1):21-28.
18. MathWorks. Web site. <http://www.mathworks.com/help/matlab/index.html>.
19. Bettega D, Calzolari P, Chauvel P. Radiobiological studies on the 65 MeV therapeutic proton beam at Nice using human tumour cells. *Int J Radiat Biol*. 2000;76(10):1297-1303.
20. Gerweck LE, Kozin SV. Relative biological effectiveness of proton beams in clinical therapy. *Radiother Oncol*. 1999;50(2): 135-142.
21. Blomquist E, Russell KR, Stenerlöw B, Montelius A, Grusell E, Carlsson J. Relative biological effectiveness of intermediate energy protons. Comparisons with ⁶⁰Co gamma radiation using two cell lines. *Radiother Oncol*. 1993;28(1):44-51.
22. Wouters BG, Lam GKY, Oelfke U, Gardey K, Durand RE, Skarsgard LD. Measurements of relative biological effectiveness of the 70 MeV proton beam at TRIUMF using Chinese hamster V79 cells and the high-precision cell sorter assay. *Radiat Res*. 1996;146(2):159-170.
23. Coutrakon G, Cortese J, Ghebremedhin A, et al. Microdosimetry spectra of the Loma Linda proton beam and relative biological effectiveness comparisons. *Med Phys*. 1997;24(9):1499-1506.
24. Robertson JB, Eaddy JM, Archambeau JO, et al. Relative biological effectiveness and microdosimetry of a mixed energy field of protons up to 200 MeV. *Adv Space Res*. 1994;14(10): 271-275.
25. Wedenberg M, Lind BK, Toma-Daşu I, Rehbinder H, Brahme A. Analytical description of the LET dependence of cell survival using the repairable-conditionally repairable damage model. *Radiat Res*. 2010;174(4):517-525.
26. Kanemoto A, Hirayama R, Moritake T, et al. RBE and OER within the spread-out Bragg peak for proton beam therapy: in vitro study at the Proton Medical Research Center at the University of Tsukuba. *J Radiat Res*. 2014;55(5):1028-1032.
27. Tang J, Inoue T, Yamazaki H, et al. Comparison of radiobiological effective depths in 65-MeV modulated proton beams. *Br J Cancer*. 1997;76(2):220-225.
28. Gueulette J, Böhm L, Slabbert JP, et al. Proton relative biological effectiveness (RBE) for survival in mice after thoracic irradiation with fractionated doses. *Int J Radiat Oncol*. 2000;47(4): 1051-1058.
29. Gueulette J, Böhm L, De Coster BM, et al. RBE variation as a function of depth in the 200-MeV proton beam produced at the National Accelerator Centre in Faure (South Africa). *Radiother Oncol*. 1997;42(3):303-309.
30. Gueulette J, Slabbert JP, Böhm L, et al. Proton RBE for early intestinal tolerance in mice after fractionated irradiation. *Radiother Oncol*. 2001;61(2):177-184.
31. Chaudhary P, Marshall TI, Perozziello FM, et al. Relative biological effectiveness variation along monoenergetic and modulated Bragg peaks of a 62-MeV therapeutic proton beam: a preclinical assessment. *Int J Radiat Oncol Biol Phys*. 2014;90(1):27-35.

32. Ando K, Furusawa Y, Suzuki M, et al. Relative biological effectiveness of the 235 MeV proton beams at the National Cancer Center Hospital East. *J Radiat Res (Tokyo)*. 2014; 42(1):79-89.
33. Urano M, Verhey LJ, Goitein M, et al. Relative biological effectiveness of modulated proton beams in various murine tissues. *Int J Radiat Oncol*. 1984;10(4):509-514.
34. McDonald MW, Wolanski JW, Simmons MR, Buchsbaum JC. Technique for sparing previously irradiated critical normal structures in salvage proton craniospinal irradiation. *Radiat Oncol*. 2013;8(1):14.
35. Wedenberg M, Toma-Dasu I. Disregarding RBE variation in treatment plan comparison may lead to bias in favor of proton plans. *Med Phys*. 2014;41(9):091706.